

Energy level alignment between 9-phosphonoanthracene self-assembled monolayers and pentacene

I. G. Hill^{a)}

Department of Physics, Dalhousie University, Halifax, Canada B3H 3J5

J. Hwang and A. Kahn

Department of Electrical Engineering, Princeton University, Princeton, New Jersey 08544

C. Huang

Department of Physics, Princeton University, Princeton, New Jersey 08544

J. E. McDermott and J. Schwartz

Department of Chemistry, Princeton University, Princeton, New Jersey 08544

(Received 4 August 2006; accepted 29 November 2006; published online 3 January 2007)

The alignment of molecular energy levels between a self-assembled monolayer of 9-phosphonoanthracene formed on silicon dioxide and pentacene has been studied using photoelectron spectroscopies. The semiconducting band gap of pentacene was found to be nested within that of the monolayer, resulting in a 1.3 ± 0.1 eV barrier for hole injection from pentacene into the monolayer. The corresponding barrier to electrons, estimated from the adiabatic highest occupied molecular orbital/lowest unoccupied molecular orbital gaps of anthracene and pentacene, is 0.3 ± 0.2 eV. Thus, the monolayer presents a significant energetic barrier to hole injection from a pentacene overlayer, but only a small to moderate barrier to electrons. © 2007 American Institute of Physics.

[DOI: 10.1063/1.2426957]

We have recently reported that organic thin film transistors (OTFTs) utilizing a self-assembled monolayer (SAM) of 9-phosphonoanthracene between the SiO₂ gate dielectric and the active pentacene layer exhibit excellent subthreshold performance.¹ The improved performance was attributed to the elimination of charge trapping states at the pentacene/SiO₂ interface, which have been previously attributed to hydroxyl groups on the SiO₂ surface.² In this work we have studied the electronic structure of the SAM and the pentacene overlayer using photoelectron spectroscopies. By learning as much as possible about its electronic structure, we hope to better understand the mechanisms behind the improved subthreshold performance.

While it seems intuitive that a well-formed SAM would eliminate these traps by binding to the SiO₂ and eliminating the surface hydroxyl groups, it is imperative that the SAM itself not act as a source of charge trapping sites. This may happen, for instance, if the electronic states of the SAM itself were strongly localized and charge from the pentacene channel was able to leak into the SAM, populating these localized states. It is therefore desirable that the SAM acts as a wide band gap insulator, with large injection barriers for both electrons and holes from the active semiconductor to the SAM. Additionally, it is also desirable that the SAM presents a surface for subsequent pentacene growth that interacts weakly with, and appears chemically similar to, the pentacene molecule. These criteria led to the choice of an anthracene-derived SAM (Fig. 1). The optical band gap of anthracene is 3.3 eV,³ compared to 1.86 eV for pentacene.⁴ Assuming that the gap of anthracene is not appreciably affected by the addition of the phosphonic acid ligand, the SAM may present appreciable barriers to both electrons and holes if the pentacene gap is nested within that of the SAM.

The conjugated π system of anthracene will present a surface for pentacene growth which is electronically similar to that of pentacene, enhancing crystalline grain formation in the pentacene overlayer.

Ultraviolet and x-ray photoelectron spectroscopies (UPS and XPS) were used to study the Si/SiO₂/SAM/pentacene system. He I and He II radiation (21.2 and 40.8 eV, respectively) were used for UPS and Mg K α (1253.6 eV) radiation was used for XPS. UPS spectra were collected with a -3 V bias applied to the sample, so that the onset of photoemission could be measured to determine the position of the surface vacuum level. All studies were performed in interconnected organic deposition (pressure $\approx 10^{-9}$ Torr) and analysis (pressure $\approx 10^{-10}$ Torr) chambers.

In order to duplicate as closely as possible the original OTFT fabrication conditions,¹ heavily doped (n type $\approx 0.001 \Omega \text{ cm}$) Si(100) wafers were used as substrates for this experiment. The OTFTs utilized a 1000 Å thick thermal SiO₂ layer as a gate dielectric. It was not possible to use such a thick oxide layer in the current experiment, as this would have led to surface charging during the photoemission studies. Instead, an ultrathin layer of approximately 7 Å was grown on the substrates using a process of oxide stripping with HF followed by reoxidation using HNO₃, as reported elsewhere.⁵ The 9-phosphonoanthracene SAMs were formed on these substrates using the procedure presented elsewhere.^{1,6} The areal density of 9-phosphonoanthracene molecules within the SAM is $\approx 2 \times 10^{14} / \text{cm}^2$, as determined by quartz crystal microbalance measurements. Pentacene was incrementally deposited on top of the SAMs at $\approx 0.1 \text{ Å/s}$. Ultraviolet photoelectron spectra were collected from the bare SiO₂ control samples, bare SAM, and at pentacene overlayer total thicknesses of 2, 4, 8, 16, 32, and 64 Å. In addition, multilayer films of the SAM precursor molecule were used to measure the ionization energy (IE) of

^{a)}Electronic mail: ian.hill@dal.ca

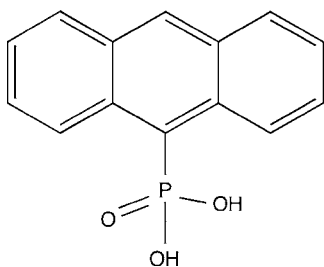


FIG. 1. SAM precursor molecule. Details of the synthesis and monolayer preparation can be found elsewhere (Refs. 1 and 6).

the SAM molecule. The photoionization cross section of the SAM highest occupied molecular orbital (HOMO) was too weak to be measured directly from the SAM surfaces, necessitating the study of these multilayer films. The thickness of these multilayer films was estimated to be ≈ 10 Å from the attenuation of the Si $2p$ core level XPS spectrum.

The UPS spectrum of a SAM-molecule multilayer is presented in Fig. 2. The position of the vacuum level was determined from the onset of photoemission. The data presented have been processed by subtracting an exponential background from the raw data, fit to the smoothly increasing spectrum on either side of the 9-phosphonoanthracene HOMO. The IE of the SAM molecule, defined by the low binding energy edge of the UPS HOMO feature, was determined to be 6.1 ± 0.1 eV. This is ≈ 0.5 eV larger than the reported IE of anthracene thin films,⁷ probably due to the influence of the phosphonic acid ligand. Note that the functional form of the background model did not influence the extracted IE within our experimental uncertainty. As the SAM HOMO is not directly observable on monolayer samples, we must assume that the IE is not significantly altered by the covalent bonding of the phosphonate group to the SiO_2 . We justify this assumption by noting that the HOMO will consist of contributions from the conjugated π system of the phenyl rings, while the substrate bonding will involve only the P–O bonds.

The UPS spectra for the bare SAM and incremental pentacene overlayer thickness are presented in Fig. 3. The left panel illustrates the evolution of the onset of photoemission (vacuum level) as a function of pentacene thickness, while the right panel indicates the evolution of the density of states

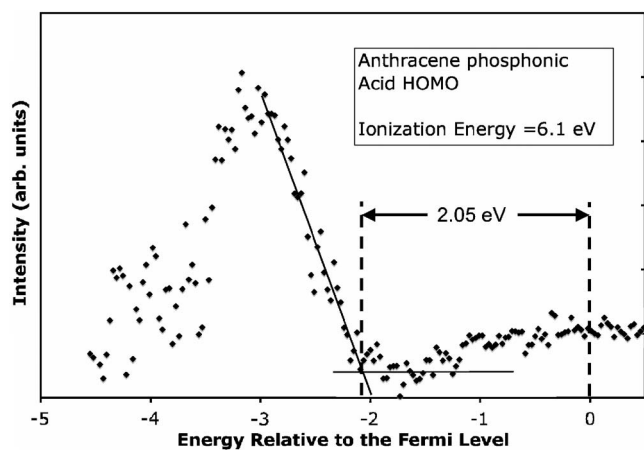


FIG. 2. UPS spectrum of the SAM highest occupied molecular orbital following background subtraction. The top of the HOMO is 2.05 eV below E_F , and the ionization energy of the molecule is 6.1 ± 0.1 eV. The position of the vacuum level was determined from the onset of photoemission (not shown).

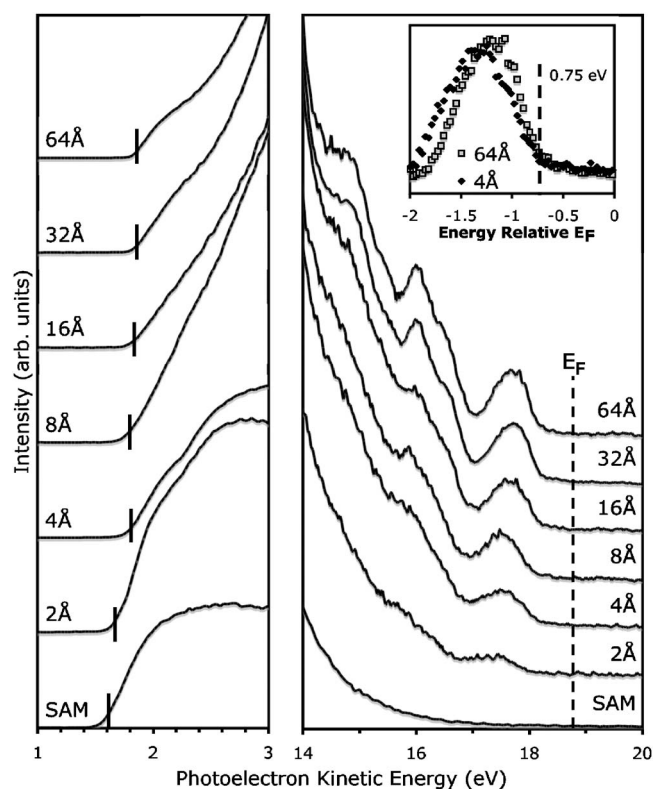


FIG. 3. Evolution of the valence density of states and the onset of photoemission for incremental deposition of pentacene on the SAM. The first molecular monolayer is completed at ≈ 16 Å. The inset shows the binding energy of the top of the HOMO relative to E_F (0.75 eV).

in the vicinity of the pentacene HOMO. The SAM-coated substrate exhibits an onset of photoemission at 1.6 eV. The onset shifts to higher kinetic energy upon pentacene deposition, saturating at 1.8 eV at a pentacene coverage of one molecular monolayer. For the usual standing-up phase of pentacene, this corresponds to a nominal thickness of ≈ 16 Å.⁵ Thus, we attribute this 0.2 eV shift to the formation of a small interface dipole between the SAM and pentacene overlayer. The evolution of the frontier orbital spectrum behaves in a similar fashion. The pentacene HOMO and other low binding energy states are clearly visible, even at a nominal coverage of 2 Å. These features grow in intensity and appear to undergo slight binding energy shifts with increasing pentacene thickness. The shifts appear to saturate at the monolayer coverage. The HOMO data for 4 and 64 Å total thicknesses are presented in the inset of Fig. 3, following background subtraction and intensity normalization. Closer examination of the HOMO feature reveals that the low binding energy edge of the peak does not move appreciably, but that at low coverages the peak is broadened and the peak maximum therefore occurs at higher binding energy. This behavior has been seen before and can be understood in terms of the evolution of the polarization screening of the photohole during the formation of the first molecular layer.^{8,9} As the monolayer is completed, the peak narrows, and its position remains constant with increasing overlayer thickness. The IE of the pentacene film is 5.0 ± 0.1 eV, in agreement with previous reports.^{10,11}

Figure 4 illustrates the alignment of energy levels in the four regions of the sample: Si, SiO_2 , SAM, and pentacene. Note that the Si and SiO_2 levels have not been directly measured in this experiment. We have assumed that the Fermi

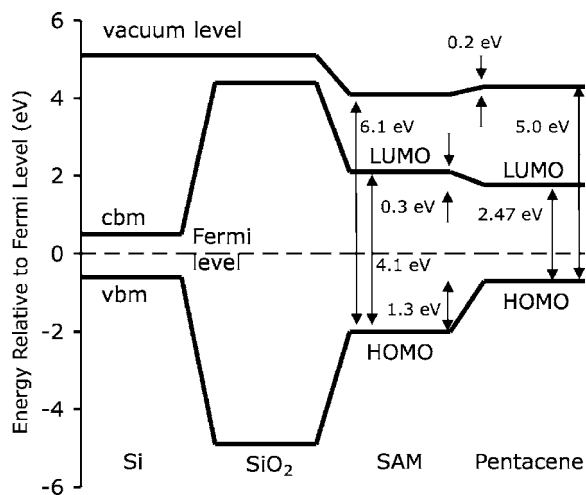


FIG. 4. Frontier energy level alignment of the Si substrate, SiO₂ dielectric, SAM, and pentacene overlayer. The SAM and pentacene LUMO levels are inferred from the measured HOMO positions, taking into account the reported adiabatic energy gaps (Ref. 3). Si/SiO₂ levels are from Ref. 12.

level is pinned 0.6 eV above the Si valence band maximum at the Si(100)/SiO₂ interface.¹² This assumption does not influence the results or conclusions reached in this study. The interface dipole of $+0.2 \pm 0.1$ eV between the 9-phosphonoanthracene SAM and pentacene, and the hole injection barrier of 1.3 ± 0.1 eV from pentacene to the SAM have been measured in this experiment. The hole injection barrier is the difference between the low binding energy edges of the SAM and pentacene HOMOs (2.05 and 0.75 eV, respectively). In order to estimate the lowest unoccupied molecular orbital (LUMO) offset between pentacene and the SAM, care must be exercised. Traditionally, optical absorption HOMO-LUMO gaps have been used to estimate the position of the electron transport LUMO level. The optical gap is smaller than the transport gap by an amount equal to the exciton binding energy, which can be large in these materials.¹³ When optical gaps are used, it is therefore implicitly assumed that the two materials comprising the heterointerface have similar exciton binding energies. This assumption is invalid in this case. The much smaller anthracene molecule constrains the electron and hole to a much smaller volume than in the case of pentacene, resulting in a significantly larger exciton binding energy. Unfortunately, these values are not well known, and reports in the literature vary by more than 0.5 eV for the same molecule, depending on the measurement technique.¹⁴ We have therefore chosen to use adiabatic energy gaps, after Silinsh and Čápek,³ derived from photoconductivity measurements of pentacene and anthracene. This ensures consistency in the estimated LUMO positions of both molecules. In constructing Fig. 4 we have used a pentacene transport gap of 2.47 eV and a 9-phosphonoanthracene transport gap of 4.1 eV.³ The electron barrier between pentacene and the SAM is estimated to be 0.3 ± 0.2 eV.

We now discuss Fig. 4 in the context of the dramatically enhanced subthreshold performance of OTFTs incorporating the 9-phosphonoanthracene SAM.¹ The current study has shown that a large barrier exists to the injection of holes, but not electrons, from pentacene into the SAM. As stated in the Introduction, it is desirable that the SAM present large injection

barriers to both electrons and holes. Furthermore, the trapping states at the SiO₂/organic interface have been attributed to electron-trapping hydroxyl groups,² and the large positive threshold voltages and poor subthreshold performance of pentacene OTFTs have been previously attributed to electron traps at the semiconductor/dielectric interface.^{15,16} It would therefore seem imperative that the SAM acts as an electron blocking layer to improve device performance. There may be other mechanisms, however, that eliminate the trapping states. The SAM may eliminate surface hydroxyl groups through the bonding of the 9-phosphonoanthracene to the SiO₂ surface. Alternately, the pentacene trap states may be created by the interaction between the first pentacene molecular layer and the bare SiO₂ surface. The presence of the SAM may prevent the formation of these interaction-induced trapping states, resulting in improved devices. It should be noted that the transport gap of anthracene phosphonic acid is not actually known—we have assumed that it is equal to that of anthracene. The phosphonic acid ligand is strongly electron withdrawing, which would tend to localize the exciton. If the exciton binding energy of anthracene phosphonic acid is closer to that of naphthalene, rather than anthracene, we may have underestimated the electron barrier by as much as 0.3 eV. Further investigation is required to determine the mechanism of trap elimination.

This work was supported by the Natural Sciences and Engineering Research Council of Canada and the Canada Foundation for Innovation (I.G.H.), the National Science Foundation (DMR-0408589) (J.S. and A.K.), the Princeton MRSEC of the National Science Foundation (DMR-0213706) (A.K.), the National Defense Science and Engineering Graduate Fellowship program (J.E.M.), and CRG Chemical of San Diego, California (I.G.H. and J.S.).

¹M. McDowell, I. G. Hill, J. E. McDermott, S. L. Bernasek, and J. Schwartz, *Appl. Phys. Lett.* **88**, 073505 (2006).

²L.-L. Chua, J. Zaumseil, J.-F. Chang, E. C.-W. Ou, P. K.-H. Ho, H. Sirringhaus, and R. H. Friend, *Nature (London)* **434**, 194 (2005).

³E. A. Silinsh and V. Čápek, *Organic Molecular Crystals: Interaction, Localization and Transport Phenomena* (American Institute of Physics, Melville, NY, 1994).

⁴M. Stella, C. Voz, J. Puigdollers, F. Rojas, M. Fonrodona, J. Escarré, J. M. Asensi, J. Bertomeu, and J. Andreu, *J. Non-Cryst. Solids* **352**, 1663 (2006).

⁵R. Ruiz, B. Nickel, N. Koch, L. C. Feldman, R. F. Haglund, A. Kahn, and G. Scoles, *Phys. Rev. B* **67**, 125406 (2003).

⁶E. L. Hanson, J. Schwartz, B. Nickel, N. Koch, and M. F. Danisman, *J. Am. Chem. Soc.* **125**, 16074 (2003).

⁷W. R. Salaneck, *Phys. Rev. Lett.* **40**, 60 (1978).

⁸I. G. Hill, A. J. Mäkinen, and Z. H. Kafafi, *Appl. Phys. Lett.* **77**, 1825 (2000).

⁹I. G. Hill, A. J. Mäkinen, and Z. H. Kafafi, *J. Appl. Phys.* **88**, 889 (2000).

¹⁰S. Kang, Y. Yi, C. Kim, S. Cho, M. Noh, K. Jeong, and C. Whang, *Synth. Met.* **156**, 32 (2006).

¹¹N. Koch, A. Kahn, J. Ghijsen, J.-J. Pireaux, J. Schwartz, R. Johnson, and A. Elschner, *Appl. Phys. Lett.* **82**, 70 (2003).

¹²F. J. Himpfel, F. R. McFeely, A. Taleb-Ibrahimi, J. A. Yarnoff, and G. Hollinger, *Phys. Rev. B* **38**, 6084 (1988).

¹³I. G. Hill, A. Kahn, Z. G. Soos, and R. A. Pascal, Jr., *Chem. Phys. Lett.* **327**, 181 (2000).

¹⁴K. Hummer and C. Ambrosch-Draxl, *Phys. Rev. B* **71**, 081202 (2005).

¹⁵A. Bolognesi, M. Berliocchi, M. Manenti, A. D. Carlo, P. Lugli, K. Lmimouni, and C. Dufour, *IEEE Trans. Electron Devices* **51**, 1997 (2004).

¹⁶G. Gu, M. G. Kane, J. E. Doty, and A. H. Firester, *Appl. Phys. Lett.* **87**, 243512 (2005).